Environmental Pollution 265 (2020) 115052

Contents lists available at ScienceDirect

Environmental Pollution

journal homepage: www.elsevier.com/locate/envpol

Comparing the performance of three methods to assess DOM dynamics within two distinct glacierized watersheds of the tropical Andes☆

K.A. Rodriguez-Avella [a, *], M. Baraer [a], B. Mark [b], J. McKenzie [c], L. Somers [c]

[a] École de technologie supérieure, University of Quebec, 1100 Notre-Dame Street West, Montreal QC H3C 1K3, Canada
[b] Department of Geography, The Ohio State University, 1036 Derby Hall, 154 North Oval Mall, Columbus, 43210-1361, United States
[c] Department of Earth and Planetary Sciences, McGill University, 3450 University Street, Montreal QC H3A 2A7, Canada

ARTICLE INFO

Article history:
Received 30 August 2019
Received in revised form
15 June 2020
Accepted 16 June 2020
Available online 22 June 2020

Keywords:
Fluorescence spectroscopy
Parallel factor analysis
Dissolved organic matter
Fluorescent dissolved organic matter
Water quality
Watershed scale

ABSTRACT

Dissolved organic matter (DOM) is recognized as a good indicator of water quality as its concentration is influenced by land use, rainwater, windborne material and anthropogenic activities. Recent technological advances make it possible to characterize fluorescent dissolved organic matter (FDOM), the fraction of DOM that fluoresces. Among these advances, portable fluorometers and benchtop fluorescence excitation and emission spectroscopy coupled with a parallel factor analysis (EEM-PARAFAC) have shown to be reliable. Despite their rising popularity, there is still a need to evaluate the extent to which these techniques can assess DOM dynamics at the watershed scale. We compare the performance of *in-situ* measurements of FDOM with laboratory measurements of fluorescence spectroscopy within the context of two distinct glacierized watersheds in Peru. Glacierized watersheds represent unique testing environments with contrasting DOM conditions, flowing from pristine, vegetation-free headwaters through locations with obvious anthropogenic influences. We used an *in-situ* fluorometer and a portable multimeter to take 38 measurements of FDOM, pH and turbidity throughout the two catchments. Additionally, samples were analyzed in the laboratory using the EEM-PARAFAC method. Results were compared to dissolved organic carbon (DOC) measurements using standard high-temperature catalytic oxidation. Our results show that the three techniques together were able to capture the DOM dynamics for both studied watersheds. Taken individually, all three methods allowed detection of the watershed DOM main points of sources but in a more limited way. Due to the narrow bandwidth of the portable fluorometer used in the study, FDOM measurements were almost non-detectable to protein-like substances. Indeed, the more demanding EEM-PARAFAC was able to both differentiate between potential sources of DOM and provide an estimate of relative concentrations of different organic components. Finally, similar to FDOM but to a lesser extent, the DOC measurements showed some limits where protein-like substances make up most of the DOM composition.

1. Introduction

The Integrated Water Resources Management (IWRM) approach is accepted internationally as the way forward for efficient, equitable and sustainable development and management of the world's limited water resources (UN-Water, 2008). Among others, IWRM incorporates water quality aspects, requiring monitoring of key water physico-chemical and biological parameters in a distributed way (Nikolaou et al., 2008; Sun et al., 2013). Among those parameters, DOM could be a proxy for capturing rapid changes in water quality and thereby provide an early warning signal for the quality of water supply (Yao et al., 2015).

DOM is a complex mixture of organic compounds like humic acids, proteins and carbohydrates (Zhao et al., 2015); it is broadly distributed in freshwater systems (e.g., Zhou et al., 2015) and plays an important role in biogeochemical processes. Among its functions, it serves as an energy source for biota and it controls and/or affects levels of dissolved oxygen, nutrients, various trace metals

☆ This paper has been recommended for acceptance by Charles Wong.
* Corresponding author.
E-mail address: Katherine.rodriguez-avella.1@ens.etsmtl.ca (K.A. Rodriguez-Avella).

https://doi.org/10.1016/j.envpol.2020.115052

and acidity (Leenheer and Croué, 2003). In addition, DOM takes part in the transport of organic and inorganic compounds (Conte and Kucerik, 2016), including pollutants, at the watershed scale (Chen et al., 2019; Derrien et al., 2019; Old et al., 2019).

DOM enters freshwater systems from different sources: allochthonous sources, which come from outside the system, and autochthonous sources, which are produced within the system, such as *in-situ* production (DeVilbiss et al., 2016; Zhou et al., 2019). Treated and/or untreated wastewater inputs contribute to allochthonous-sourced DOM and are linked to anthropogenic activities (Tang et al., 2019). As such, DOM can be used to trace the source, species and migration of contaminants (Peng et al., 2018), making it an excellent water quality indicator. In recent decades, climate change, eutrophication and human activities have contributed to an increase in the inputs of terrestrial DOM to aquatic ecosystems (Massicotte et al., 2017), making it important to understand DOM dynamics at the watershed scale. However, the characterization of aquatic organic matter remains challenging because it is the result of a mixture of organic compounds from different sources and processes that require different analytical approaches (Coble et al., 2014). There are several proxies that can be used to characterize DOM. Since carbon represents approximately 65% of the elements in DOM (Bolan et al., 2011), it is common to express DOM as DOC (Qualls et al., 2013). DOC is considered a reliable proxy for DOM quantity, considering the molecular complexity found in the dissolved organic load (Thurman, 1985). An alternate method for characterizing DOM is measuring FDOM. FDOM is the fraction of chromophoric DOM (CDOM) that fluoresces as it releases absorbed energy at a different wavelength from the absorbed one. One of the operational distinctions that can be made for FDOM is between two fluorescent signals: protein-like fluorescence and humic-like fluorescence (Coble, 1996). Protein-like fluorescence includes the three fluorescent aromatic amino acids: phenylalanine, tyrosine and tryptophan (Lakowicz, 2006). Humic-like fluorescence corresponds to signals of humic substances that arise from the breakdown and decomposition of vascular plants (Anesio et al., 2005; Stedmon et al., 2003).

Various techniques exist for measuring DOC, including spectrophotometry, wet oxidation, dry combustion and molecular weight fractions (Bolan et al., 2011). The method that uses high-temperature catalytic oxidation (Sugimura and Suzuki, 1988), improved by Suzuki et al. (1992), is one of the most popular amongst the scientific community. Although DOC measurements are widely used, they can be expensive (Chatterjee et al., 2009), and methods that employ chemical oxidation are limited by incomplete oxidation of protein-like molecules, which affects their accuracy. Other disadvantages of these methods are that sample contamination can occur from using reagents (Bisutti et al., 2004), and the lag time between sample collection and processing, plus storage conditions, can lead to biased results due to the effects of degradation.

Measuring FDOM accounts for approximately only 1% of DOM (Cory et al., 2011), but it has the advantage of being non-destructive and requiring little time and preparation. Fluorescence occurs at specific excitation and emission wavelengths, depending on the compounds building FDOM, and the intensity of the signal has been shown to be proportional to concentration (Cory et al., 2011; Fellman et al., 2010). Monitoring DOM using fluorescence measurements is appealing because it is a fast and reagent-free technique that entails no sample preparation (Henderson et al., 2009), it is very precise in its measurements, and it has a reasonable cost (Lee et al., 2018). In addition, DOM associated with sewage has given rise to consideration of fluorescence as a reliable alternative to standing water quality parameters due to the strong fluorescence signal that it provides (Tang et al., 2019).

In-situ optical sensing using fluorescence is one of the FDOM measurement techniques that has seen increased usage due to technical advances and cost reduction (Blaen et al., 2016). Employing fluorometers or equipping multiparameter sondes with fluorescence sensors also allows for continuous quantification of DOM changes through time. Among the studies using these techniques, Bridgeman et al. (2011) developed and deployed a novel, LED-based instrument capable of detecting peaks that are surrogates of organic and microbial matter. Recently, Carstea et al. (2016) proposed a review of the advances in *in-situ* fluorescence measurements. One of the interesting characteristics of the method is that it does not require sample manipulation, transportation or conservation, which is a clear advantage given the inherent instability of labile organic components (Hansen et al., 2016). However, temperature and turbidity corrections are potentially required (Downing et al., 2012; Saraceno et al., 2017; Watras et al., 2011).

Fluorescence spectroscopy, a relatively recent technique, generates three-dimensional excitation and emission matrices (EEMs). This benchtop technique has been widely used to identify sources and compositions of fluorescent DOM in natural watersheds (Zhang and Liang, 2019). A growing number of studies have applied parallel factor analysis (PARAFAC) for EEM interpretation (Baghoth et al., 2011; Coble, 1996; Coble et al., 2014; Murphy et al., 2011, 2013; Stedmon et al., 2003; Yamashita and Jaffé, 2008). PARAFAC decomposes the EEMs into individual fluorescent components (Weiwei et al., 2019) and has been effectively used to recognize and differentiate allochthonous and/or autochthonous fluorescent DOM components in various aquatic environments (Henderson et al., 2009).

Despite the recent rise in applications of fluorescence-based techniques for monitoring DOM, there is still a need to further assess the limits of measuring FDOM to characterize the DOM dynamics at the watershed scale. Among others, Lee et al. (2015) compared UV-VIS and FDOM sensors for *in-situ* monitoring; Khamis et al. (2015) compared the performances of two field deployable sensors with the objective of better understanding the interference of temperature and turbidity in tryptophan-like fluorescence; Baker et al. (2004) compared the performances of two portable protein-like sensors with the results of a bench-top spectrophotometer; Carstea et al. (2016) compared results measured in real time vs. control samples in a spectrofluorometer in a mobile laboratory; and Wasswa et al. (2019) compared the performance of portable sensors and benchtop fluorometers in control samples and samples from different stages of a water reuse facility.

In the present study, measurements from *in-situ* optical FDOM sensors, benchtop fluorescence spectroscopy and high-temperature combustion DOC analysis are compared for 38 sampling locations spread over two mesoscale glacierized catchments in the Peruvian Andes. The watersheds were selected because they present high spatial variability in DOM sources and concentration, and because they flow from pristine mineral headwaters to points of obvious anthropogenic influence. Using DOC as reference, the objective of this study is to evaluate the performance of the proposed fluorometric methods in capturing DOM dynamics for watershed management.

2. Materials and methods

2.1. Study sites

The Shullcas and Santa Rivers both drain glacierized watersheds situated in the Peruvian Andes (Fig. 1). The region is characterized

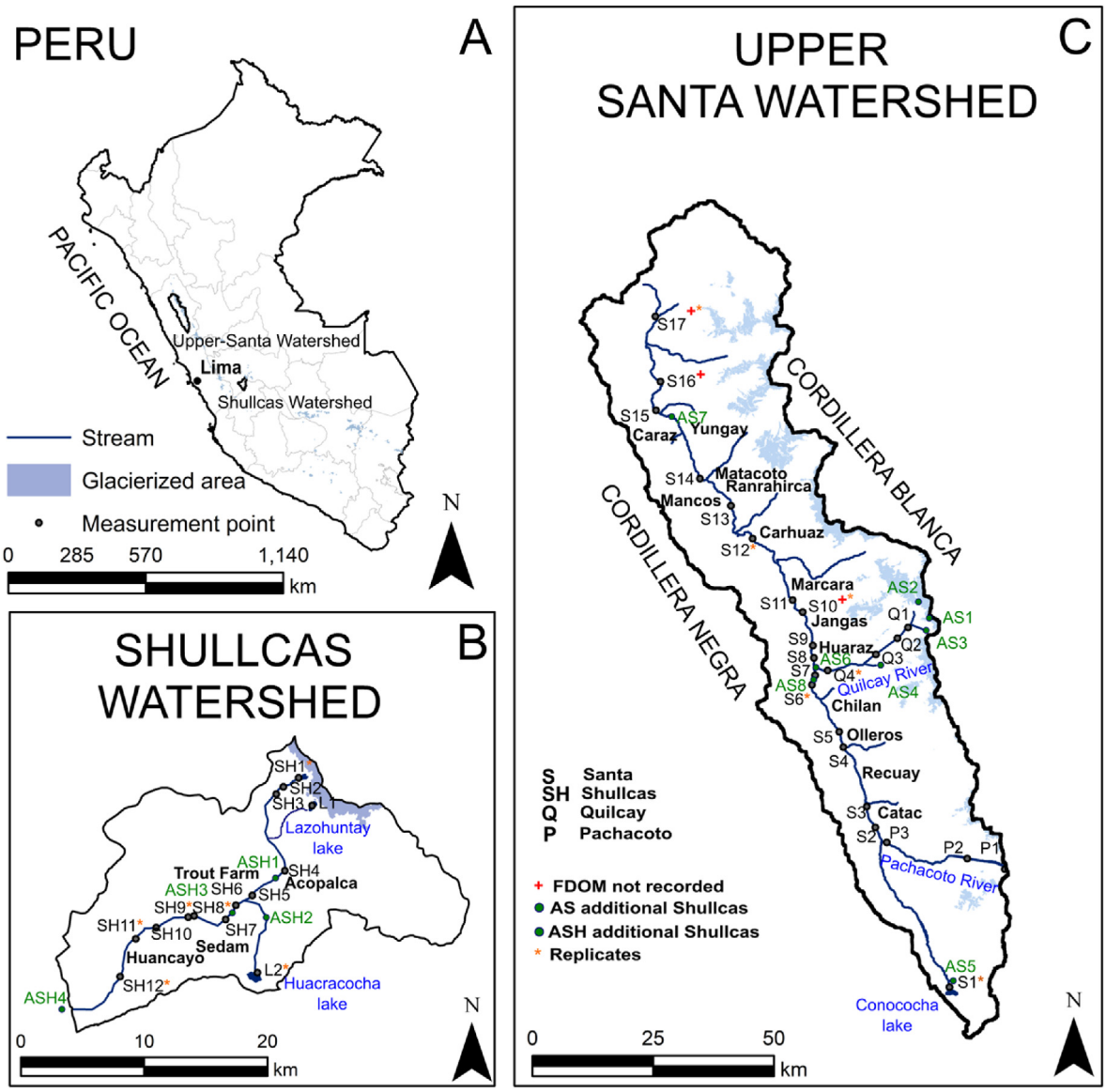

Fig. 1. A. Map of Peru indicating location of study watersheds. B. Shullcas watershed. C. Upper Santa watershed. Glacierized areas are shaded in grey, sampling points are located using black dots. Sample sites and major cities' names are in black while water bodies' names are in blue. (For interpretation of the references to colour in this figure legend, the reader is referred to the Web version of this article.)

by strong seasonality in precipitation, with almost no rain during the dry season and abundant rainfall during the austral summer (Garreaud, 2009). Dry season conditions are favorable for synoptic sampling of mesoscale watersheds because glacier melt's contribution to base flow is predominant over that of precipitation runoff (Mark et al., 2005).

Both rivers flow from glacial origin headwaters through naturally vegetated valleys. Progressively, both rivers pass several villages and agricultural areas, where settlement density increases, and the rivers are impacted by anthropogenic activities and contamination by untreated wastewater.

As the glaciers in the Peruvian Andes retreat, the decrease in meltwater is predicted to lead to a significant decline in river discharge in the coming decades, particularly during the dry season (Baraer et al., 2012), and this is raising concerns about water quality (Guittard et al., 2017). Overall, these factors motivated the selection of these study sites for evaluating and comparing DOC and FDOM measurements.

2.1.1. Shullcas watershed

The Shullcas watershed is located upstream of the city of Huancayo (Fig. 1B). It flows from the Chuspicocha and Lasohuntay proglacial lakes, located on the western side of the glacierized Huaytapallana Mountain, with a peak elevation of 5557 m.a.s.l. The Huaytapallana glaciers currently cover 22 km^2 but lost 56% of their total surface area between 1984 and 2011 (López-Moreno et al., 2014). The Shullcas River flows through several villages, agricultural areas and trout farms before reaching Huancayo. The population density increases progressively until the river reaches Huancayo (pop. 470,000).

2.1.2. Upper Santa watershed

The Santa River drains the western slopes of the Cordillera Blanca, a mountain chain with the highest density of tropical glaciers in the world (Fig. 1C). The river flows from Lake Conococha at the southern end of the watershed into the Pacific Ocean (Baraer et al., 2015).

During the dry season, meltwater represents more than 30% of the total runoff in the upper Santa River watershed (Baraer et al., 2012; Mark et al., 2005). The river receives water from glacierized tributaries such as the Quilcay (17% glacierized in 1997) and Pachacoto (8% glacierized in 1997) (Mark and Seltzer, 2003) and provides water for stakeholder and industrial agriculture, mining, domestic water and hydropower production (Gurgiser et al., 2016). The glacierized headwaters of the tributaries are above 5000 m.a.s.l. and are not impacted by significant human settlements. None of the cities along the upper Santa River are equipped with proper sewage treatment plants, and most discharge wastewater directly into the Santa River (Guittard et al., 2017), making the lower portion of the Santa an anthropogenically impacted river.

2.2. Method

2.2.1. Sampling overview and in-situ measurements

Both basins were visited with the aim of gaining a good representation of the DOM dynamics at the scale of the watershed. Water sources such as glaciers and lakes were therefore targeted, as were locations along the main stream that allowed the evolution of DOM concentration to be captured as it flows from the sources to the watershed outlets. Particular attention was paid to spots such as large cities, trout farms and confluences with major tributaries as those could affect DOM concentration in the main stream. Field observations, including around the measurement/sampling points, land use and visual watershed characteristics were recorded during the whole sampling campaign.

At most of the sampling points, FDOM, turbidity pH and stream temperature were measured onsite and a sample was taken for laboratory analysis for DOC and for EEM-PARAFAC analysis. Exceptions, detailed in the following section, are made for sampling points where FDOM measurements have not been recorded adequately, where sample replicates have been taken, or where samples have been taken for the EEM-PARAFAC model creation only.

Water samples were collected and filtered using a 0.45 μm filter. Samples were placed in sealed 60 ml HDPE amber bottles and stored at 4 °C until laboratory analysis, which occurred within four months maximum of the collection date.

We measured FDOM using a C3-Turner Designs Submersible Fluorometer. The FDOM sensor has wavelengths of 325 nm ± 60 nm for excitation and 470 nm ± 30 nm for emission. The C3 was calibrated using a standard solution prior to the sampling campaign. A solid secondary standard was used in the field on a daily basis to check any loss in sensitivity or stability. The fluorometer was submerged in the water at each site for a minimum of five minutes, with a 30-second sampling interval. Turbidity, temperature and pH were measured using a portable multiparameter probe.

2.2.2. Watersheds sampling plan

Field activities at the Shullcas watershed took place between June 29 and July 2, 2017. Twenty sampling points were visited over those four days for a total collection of 33 samples (Fig. 1b). At 14 sites (labelled SH for Shullcas and L for lake), both *in-situ* measurements, and COD and EEM-PARAFAC samples were collected. Those are used for the comparison between the three analytical methods at the scale of the Shullcas watershed. As a large set of samples will result in more components identified by the PARAFAC model (Murphy et al., 2013), the model was built using five additional sampling points (labelled ASH for Additional Shullcas) and 13 replicates.

Field activities at the Santa watershed were conducted between June 21 and June 27, 2017. A total of 32 sampling points were visited over the seven-day period (Fig. 1c.). At 24 spots (labelled S for Santa, P for Pachacoto and Q for Quilcay), both *in-situ* measurements, and COD and EEM-PARAFAC samples were collected. Unfortunately, FDOM measurement records were lost for three of those spots. The three analytical methods are compared to each other at the scale of the Santa watershed based on those sampling points. As for the Shullcas watershed, the Santa EEM-PARAFAC model was built using additional sampling spots (labelled AS for Additional Santa). In addition to the eight AS samples, a total of 16 replicates were used for that purpose.

2.2.3. Data processing for in-situ measurements

Readings from the C3 fluorometer were first preprocessed. The highest, lowest, first and last readings per site were considered as potential outliers and were erased from the records. The remaining values were averaged to obtain a unique value of uncorrected FDOM. Previous studies have shown that temperature (Wasswa and Mladenov, 2018; Watras et al., 2011) and turbidity (Downing et al., 2012; Saraceno et al., 2017) can affect optical measurements due to thermal quenching and light scattering. Turbidity under 50 NTU has, however, been shown to affect FDOM measurement by 10–20% maximum (Saraceno et al., 2017). In the absence of a well-defined protocol for post-treatment correction of FDOM value based on turbidity in the absence of granulometric measurements (Saraceno et al., 2017), and considering that the turbidity measured onsite was 24.66 NTU on average, with a standard deviation of 23.95 NTU, it was decided not to proceed with a correction on that parameter. Indeed, a 10% to 20% variation in FDOM concentration would be too low to affect the overall conclusions of the study. Raw FDOM values were corrected for temperature following Watras et al. (2011), leading to individual value adjustments ranging from 3% to 9%.

2.2.4. DOC laboratory measurements

Filtered water samples were analyzed for DOC concentration using an Apollo 9000 TOC analyzer (high-temperature catalytic oxidation method). Each sample was first acidified and sparged to eliminate inorganic dissolved carbon. It was then transferred to a quartz cell and heated at 700 °C so that all of the organic carbon was transformed to CO_2, which was quantified using infrared absorbance. The mean of the three readings is reported for every sample. Prior to analysis, a calibration curve was obtained using potassium hydrogen phthalate.

2.2.5. Fluorescence spectroscopy and generation of EEM matrices

EEMs were generated for each sample using a Cary Eclipse fluorescence spectrophotometer. Slits were set to 5 nm for excitation and emission. With the objective of obtaining EEMs, the excitation wavelength was set from 290 nm to 455 nm, and the emission wavelength from 250 to 455 nm, using a testing speed of 1200 nm/s. Eight samples selected randomly from the Shullcas River and 15 from the Santa River were tested twice in order to verify the replicability of the method. Since pure water has a clear scatter peak (i.e., the Raman peak) that can alter the fluorescence response (Cross et al., 1937; Lawaetz and Stedmon, 2009), an emission spectrum of blanks was performed every day the equipment was used. This Raman test was performed on Nanopure water using an excitation wavelength of 275 nm and an emission spectrum of 285–450 nm with 1 nm intervals. After the Raman signal was subtracted from the sample EEMs, it was then normalized and expressed in Raman units (R.U., nm^{-1}).

EEMs were corrected for possible systematic biases due to variations and/or imperfections in the optical components that could end up distorting the data and the validation of the PARAFAC that was carried out later. This was achieved by multiplying each EEM by a correction matrix specific to the instrument. The Raman peak

was also removed using the drEEM MATLAB toolbox (Murphy et al., 2013). As no samples were taken directly from sewage, no correction for the inner filter was performed. The error associated with the inner filter being at most 10% for the most concentrated samples (Lakowicz, 2006), it is assumed that the research conclusions are not affected by this effect.

2.2.6. PARAFAC modeling

For each watershed, a parallel factor analysis was applied to the corrected EEMs to decompose the spectra into their various components. As described earlier, extra samples were used to produce the PARAFAC models, making a total of 48 samples for Santa and 33 for Shullcas. This multi-way statistical data analysis is used to describe data with more than two dimensions. This analysis is known to have a 'second order advantage' (Booksh and Kowalski, 1994), meaning that the algorithm is mathematically able to separate any possible spectrally overlapping data from the EEMs into fluorescence-independent chemical components (Stedmon et al., 2003). The application of the PARAFAC approach includes spectral correction, calibration, removal of scatter, identification and removal of outliers, and model validation (Stedmon and Bro, 2008). The PARAFAC method was applied following the procedure recommended by Murphy et al. (2013) using MATLAB R2017B. Model validation was performed by conducting a split analysis that consisted of generating different models from subsample groups. The model for the entire dataset was validated, including when the loadings from the various subgroups were identical to the one from the entire dataset (Murphy et al., 2013). The components identified through PARAFAC were classified as humic-like or protein-like substances based on components with similar spectra identified in previous studies (Baghoth et al., 2011; Bridgeman et al., 2011; Coble, 1996; Stedmon and Markager, 2005; Yamashita and Jaffé, 2008; Zhao et al., 2015). The relative concentration of components was estimated by considering the maximum peak intensity (Fmax) and was expressed in Raman units (R.U., nm^{-1}).

3. Results

3.1. Shullcas watershed

Fig. 2 presents a synthesis of analytical results for the Shullcas watershed. DOC, FDOM (in situ) and EEM-PARAFAC results are presented on a single graph to facilitate comparison. Results for each analytical technique are discussed individually, followed by the performance comparison.

3.1.1. DOC measurements

DOC measurements vary from 380 ppb at the headwaters to ~4500 ppb at Huancayo. DOC concentration increases gradually as we move away from the proglacial lakes to SH7, a sampling point situated in the middle of the catchment, where it reaches 1100 ppb. Between SH7 and SH10, DOC declines slightly, reaching 780 ppb at the entrance to the urban area. DOC then shows an exponential increase from SH10 to SH12, where it reaches 4500 ppb.

The increase in DOC throughout the river's journey corresponds to land cover and land use changes according to field observations. In the absence of human activities, and with very limited vegetation cover, proglacial lake areas accumulate glacier meltwater and do not show obvious signs of intense biological activities. As the river flows through the watershed, the vegetation coverage and pastoral and agricultural activities gradually increase. Downstream of point SH5, the river passes through the village of Acopalca and a trout farm, where it shows an increase in DOC. The effect of mixing with major tributaries is observed twice in the upper watershed. Firstly, DOC shows no increase downstream of the confluence with the stream that flows from the Lasohuntay proglacial lake, where the lowest value of the entire watershed was measured (220 ppb). Several kilometres downstream, the DOC of the Shullcas River shows an increase immediately downstream of the confluence with the stream that flows out of Huacracocha Lake, in which the highest DOC value of the watershed was measured (5750 ppb). This value responds to herding and fishing activities, some shepherd settlements, and the organic-rich soil surrounding the lake.

The slight decreasing trend in DOC observed between SH7 and SH10 is mostly due to the SH7–SH8 drop. Several hypotheses are proposed for this: the absence of major settlements, possible groundwater discharge, and dilution by numerous small confluents. The slight increase in DOC observed between points SH8 and SH9 can be explained by the water use of the major trout farm. Points SH11 and SH12 are situated in the urbanized area of the watershed. Numerous points of wastewater input can be observed within that area, and various indications of water pollution were noticed at sampling (e.g., turbidity, colour, smell). This was especially the case at point SH12, where DOC reached 4500 ppb.

3.1.2. In-situ FDOM measurements

The FDOM profile of the Shullcas River closely reproduces the DOC profile (Fig. 2). FDOM readings vary from 0 ppb to 405 ppb. Like those for DOC, FDOM measurements fit well with qualitative land use observations. Few discrepancies exist between DOC and FDOM. The *in-situ* FDOM readings at Huacracocha Lake yield a concentration of 90 ppb, which is far from the highest concentration for the watershed (405 ppb at SH12). Noticeably, the Lasohuntay Lake (L1) *in-situ* FDOM measurement was 0 ppb, which suggests that there is no presence of any fluorescence component, or that the value is below the detection limit of the equipment.

3.1.3. EEM-PARAFAC

Three fluorescent components were identified and validated through the EEM-PARAFAC analysis for the Shullcas basin. Fig. 3a–c shows the contour plots for each of the different components. Component one (C1) comprises two peaks with maximal excitation at 255 and 360 nm and an emission range of 485–530 nm. Component two (C2) has a fingerprint comparable to C1's, with slightly lower emission values. It shows two peaks with maximal excitation of 260 nm and 310 nm and an emission peak maximum of 435. Component 3 (C3) shows a single peak of excitation at 285 nm and a single peak of emission at 330 nm.

Table 1 provides excitation and emission wavelengths of the main peaks for each component identified by the EEM-PARAFAC analysis, along with wavelengths of comparable components found in the literature and their possible sources.

According to the EEM-PARAFAC results, the Shullcas River's FDOM comprises two main humic-like substance groups, C1 and C2, probably of terrestrial origin, and one substance group, C3, identified as similar to tryptophan, an amino acid that is often associated with the presence of microbial activity like what is found in wastewater.

The Fmax intensities are reported in Fig. 2 for components of the PARAFAC model grouped in humic (C1+C2) and protein (C3)-like categories. For comparison with the other method, the sum of the Fmax values of the three components (SFmax) is assumed to be proportional to the overall DOM concentration. Fig. 2 describes a visual agreement between the SFmax, DOC and FDOM measurements.

Two sampling points represent exceptions to the general agreement within the three tested methods: SH4 and SH9. The EEM-PARAFAC method shows that SH4 has the second-highest total fluorescence within the SH1–SH7 transect, while the DOC

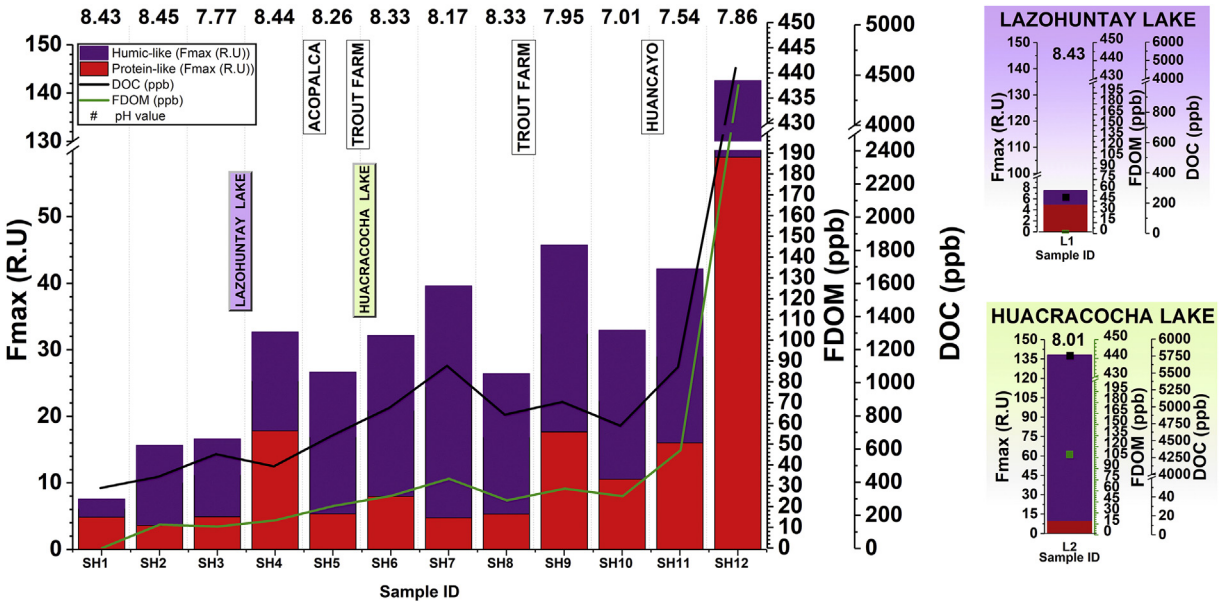

Fig. 2. Analytical results for the Shullcas watershed. DOC is shown as a black line and points. FDOM is shown in green. PARAFAC components Fmax appear as bar graphs where purple corresponds Humic-like, and red to protein-like. Names in the boxes indicate cities and tributaries. Site locations are shown in Fig. 1b. (For interpretation of the references to colour in this figure legend, the reader is referred to the Web version of this article.)

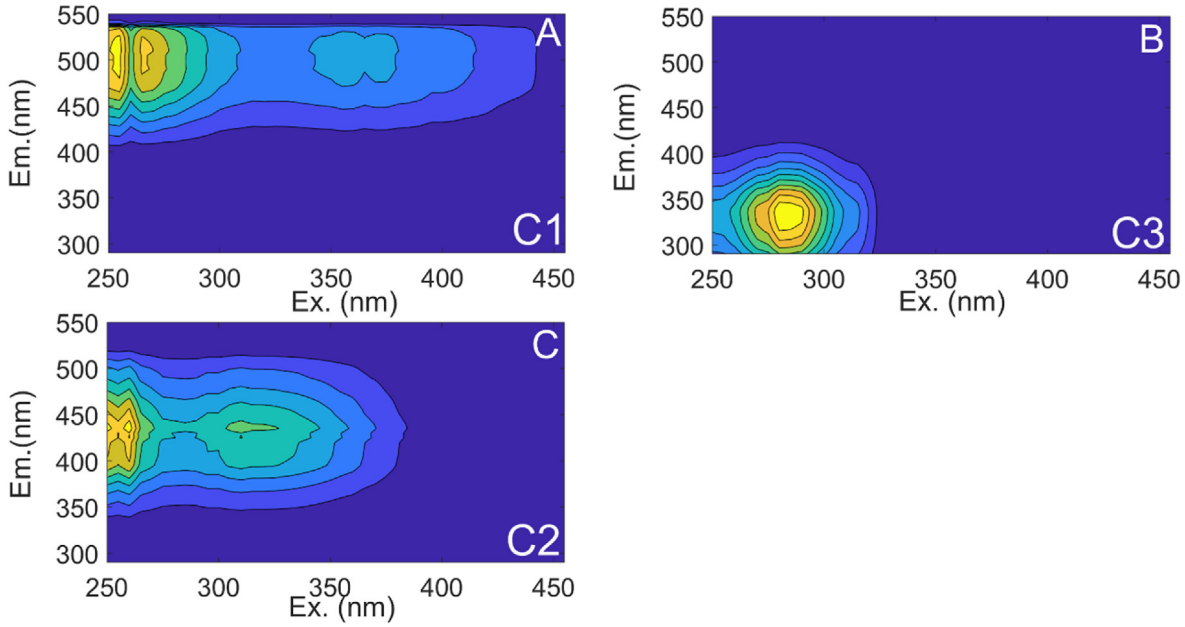

Fig. 3. Three different components of FDOM identified in the PARAFAC model for the Shullcas basin.

Table 1
Components identified in this study for the Shullcas basin with the corresponding wavelength position of its maximal fluorescence. Possible source is based on components identified in previous studies.

Component	λ (nm) (Ex/Em)	λ (nm) of possible analogue (Ex/Em)	Possible Source	Reference
C1	255(360)/485–530	237–260/400–500	Humic	Bridgeman et al. (2011)
		250(385)/504	Fulvic acid terrestrial or autochthonous	Stedmon and Markager (2005)
		260(360)/480	Terrestrial Humic Substances	Baghoth et al. (2011)
C2	260(310)/435	260/380–460	Humic-like	Coble (1996)
		237–260/400–500	Humic	Bridgeman et al. (2011)
		250(340)/440	Terrestrial humic substances	Baghoth et al. (2011)
C3	285/330	275/340	Tryptophan-like, protein-like	Coble (1996)
		275/340	Tryptophan	Bridgeman et al. (2011)
		280/344	Tryptophan-like, autochthonous	Stedmon and Markager (2005)

and FDOM measurements rank fourth and fifth, respectively. Comparably, the EEM-PARAFAC method situates the fluorescence level at SH9, proportionally higher than the two other methods. Interestingly, in both cases, the high SFmax values are associated with a particularly high protein-like substances signal. SH4 is situated just downstream of the confluence with the stream that drains the Lasohuntay Lake, which also shows a relatively high protein-like substances signal. Similarly, the trout farm, whose impact can be assessed by the two nearby points SH8 and SH9, appears to be increasing the load of protein-like substances in the main stream.

EEM-PARAFAC provides additional information to the DOC and FDOM measurements. This is the case at SH12, within the city of Huancayo, where we observe high values for all three components, suggesting diverse sources of DOM at that point. At the confluence with the stream flowing from Huacracocha Lake, EEM-PARAFAC shows a humic origin in the increase of FDOM at SH6 and SH7, the same type of component that appears to be the origin of the high fluorescence within the lake.

3.1.4. Regression study

A linear regression study is performed on the Shullcas River dataset to further explore the relation between the three different methods. Prior to computing regression parameters, we performed a Cook's distance test (Cook, 1977) with a threshold of 1 (Heiberger and Holland, 2004). Indeed, Fig. 2 shows that, for all methods, at least one point exhibits very high DOM concentrations compared to the others, making it potentially overly influential. Such points have been shown to reduce the validity of the regression results (Yuan and Zhong, 2008). With a Cook's distance of 359.5, SH12 was found to be the only one that matched the overly influential point criteria. Regression results, made of the regression line slope x_1, the intercept *int*, the coefficient of determination R^2 and its associated p-value, are therefore provided excluding SH12 and including it for reference (Fig. 6).

Fig. 6, a), c) and e), which presents regression results for the Shullcas watershed, confirms SH12 as a highly influential point. Regression performed including SH12 presents all R^2 values over 0.85 with p-values under 0.05. The situation is different for calculations performed excluding that point. SFmax values still correlate significantly (p-value = 0.002) with DOC but at a lower degree (R^2 = 0.69) than the precedent (Fig. 6a). When humic-like substances only are considered, the coefficient of determination reaches 0.86 (p-value = 3.7 10^{-5}), close to the 0.94 obtained when considering SH12 in the calculation. The situation is the opposite when protein-like substances only are considered. The statistically insignificant R^2 situates at 0.07 in that case. Even if lower than calculated when considering SH12 (Fig. 6c), the level of correlation excluding that point is still high between COD and FDOM as indicated by an R^2 at 0.89 (p-value = 2 10^{-5}). When FDOM and Fmax values are compared to each other (Fig. 6e) we observe a situation comparable to the one met with Fmax values and DOC. The highest coefficient of determination when SH12 is excluded is reached with humic-like substances and FDOM (R^2 = 0.76; p-value = 4.6 10^{-4}), closely followed by SFmax with FDOM (R^2 = 0.76; p-value = 5.8 10^{-4}). No significant correlation was found between FDOM when protein-like substances only are considered (R^2 = 0.19; p-value = 0.18). Interestingly, slopes of the regression lines differ by up to 3-fold when SH12 is excluded from those that include that point, suggesting that spots of high DOM concentration have great influence on the relationship between the different methods.

3.2. Santa watershed

A synthesis of analytical results for the upper Santa watershed is presented in Fig. 4.

3.2.1. DOC measurements

The highest recorded concentration was measured at S1 (Lake Conococha, 940 ppb), at the headwaters of the Santa River. The shallow lake, a refuge for migratory birds and regularly visited by livestock, collects wastewater from nearby human settlements. Downstream from Conococha lake, the Santa River presents a fluctuating DOC with a net negative trend as it flows through the upper watershed. Peaks are observed downstream of the city of Huaraz (S8), near Jangas (S11) and upstream of the city of Caraz.

The most pronounced drop in DOC is observed between S1 and S2, downstream of Lake Conococha. The Santa River collects water from the west side of the Cordillera Blanca, where glacier meltwater is a large component of the dry season discharge. The Pachacoto River, a glacierized tributary, flows from a proglacial lake that has the lowest DOC value (62 ppb; P1) measured in the upper Santa watershed and joins the Santa River between S1 and S2. As the Pachacoto River flows to the Santa River, it passes through pasture lands and small settlements, and its DOC concentration increases to 600 ppb at P2 and 476 ppb at P3.

From S2 to S5, DOC is relatively stable. Point S5 is just downstream of the confluence with the Rio Negro and is the DOC minimum for the river (980 ppb). DOC increases between S5 and S8 (2150 ppb), with the latter being downstream of Huaraz, just downstream of the confluence with the Quilcay River (Q1 to Q4). Similar to Pachacoto, the Quilcay tributary originates from proglacial lakes. DOC concentrations at Quilcay vary between 150 and 200 ppb, with the highest value being recorded furthest downstream at Q4, just upstream of Huaraz.

Downstream of Huaraz, DOC in the Santa River decreases slightly as the population density decreases (S9 and S10) and several tributaries join the main river. DOC increases again at S11 in Jangas, to almost 2200 ppb, which corresponds to field observations that describe the site as trash-laden and having a bad odour. From Jangas, DOC gradually decreases, reaching a minimum at S17 at the hydropower facility river intake. Declining DOC in this portion of the river occurs simultaneously with large tributary inflows and limited human activities as the river incises and the valley slopes become steeper. Except for the DOC peak at S11, DOC variations match field observations of urbanization and watershed dynamics.

3.2.2. In-situ FDOM measurements

The FDOM profile of the Santa River closely mimics that of DOC between S1 and S9. The highest FDOM value was measured in Lake Conococha (155 ppb). FDOM then drops to 40 ppb, possibly due to the presence of a tributary. The FDOM spatial variability along the Pachacoto River has a similar pattern to the DOC, with the difference being that the P1 FDOM is 0 ppb, suggesting the proglacial lake is free of organic matter. Along the Santa River, FDOM peaks to a value of 57 ppb just downstream of Huaraz and at the confluence of the Quilcay River (S8), similar in pattern to DOC. The Quilcay River has 0 ppb for points Q1 to Q3, like the Shullcas watershed, suggesting that proglacial lakes do not have significant biological activities and confirming the DOC measurement. The last sampling point on the Quilcay River (Q4) shows a slight increase in FDOM to 2 ppb.

Immediately downstream of S8 in the Santa River, FDOM decreases slightly along with DOC, to 52 ppb. Unfortunately, the measurement results are not available for S10, S16 or S17 due to equipment failure. Between S12 and S15, the FDOM curve does not mimic the DOC, particularly between S14 and S15, where there are opposite trends.

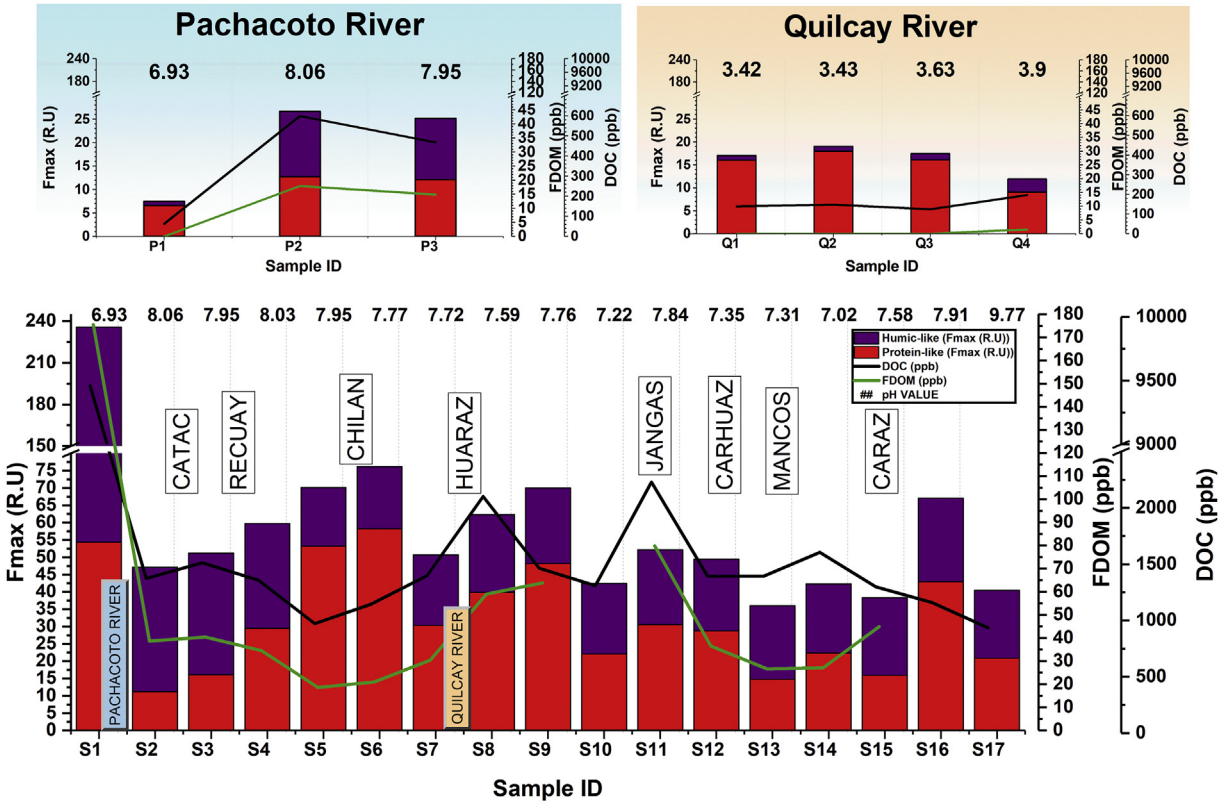

Fig. 4. Analytical results for Upper Santa watershed. DOC is shown as a black line and points. FDOM is shown in green. PARAFAC components Fmax appear as bar graphs where purple corresponds Humic-like and red represents protein-like. (For interpretation of the references to colour in this figure legend, the reader is referred to the Web version of this article.)

3.2.3. EEM-PARAFAC

After subtracting the Raman signal and normalizing the data, four fluorescent components were identified for the upper Santa watershed using the EEM-PARAFAC analysis. Fig. 5a–d shows the contour plots for each of the different components. Component one (C1) has an Fmax excitation wavelength of 255 nm, with an emission ranging from 440 to 490 nm (Fig. 5a). Components two (C2), three (C3) and four (C4) exhibit peak excitation wavelengths of 295, 265–280 and less than 250 nm, respectively, while their peak emission wavelengths are 335–360, 320–350 and 350 nm (Fig. 5b, c and d, respectively).

As in the Shullcas study, the spectral characteristics of the four

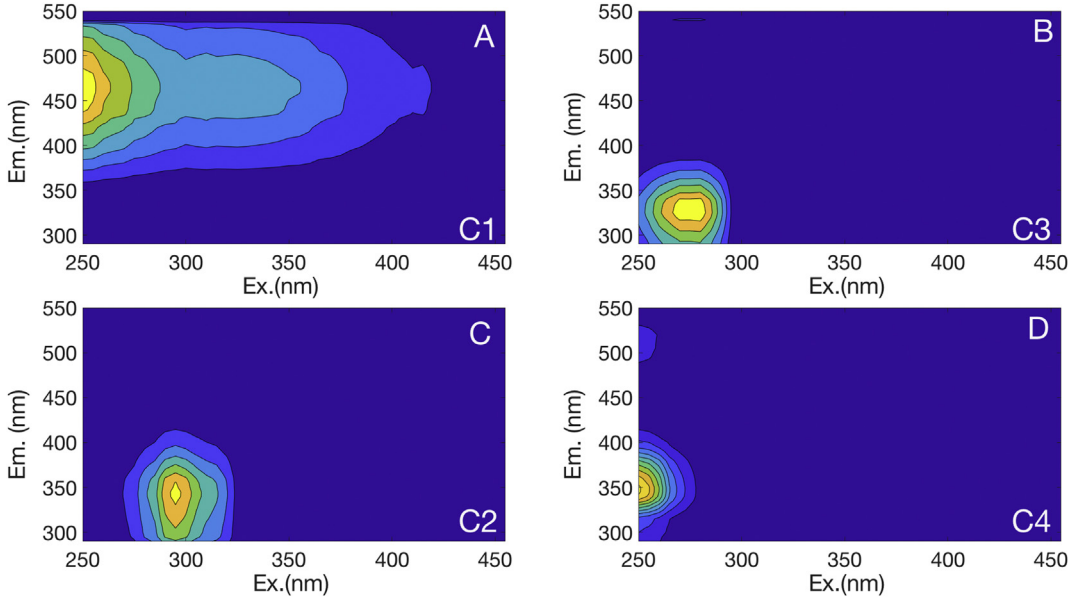

Fig. 5. a-d. Four different components identified in the PARAFAC model for the Santa basin.

components were then compared to those of components described in the literature for the excitation and emission wavelength positions of the peaks (Table 2).

The EEM-PARAFAC results from the Santa basin contain one component that corresponds to humic-like substances (C1) and three components whose fingerprints correspond to protein-like substances (C2, C3, C4). The evolution of the components along the rivers is shown as bars in Fig. 4.

That figure shows that, from S1 to S3, the three methods have similar trends of DOM. In the same area, samples taken in the Pachacoto River produce good agreement among the three methods. Starting at S4, we observe differences in the concentration profiles among the three detection methods. The most noticeable differences between the EEM-PARAFAC, DOC and FDOM profiles in the Santa River occur between S4 and S9, where EEM-PARAFAC shows a gradual increase of fluorescence, reaching a peak just downstream of Chilan, which marks the beginning of the Huaraz urban area. A drop in DOM is then observed at S7, the most upstream sample taken in the Huaraz region. This method situates the peak in DOM associated with the city of Huaraz fingerprint at S9, 4 km downstream of S8, where the DOC method measured its maximum value for the Huaraz urban area.

Unlike the DOC method, the EEM-PARAFAC method does not identify Jangas (S11) as a particularly high DOM hotspot. Finally, the EEM-PARAFAC method suggests a particularly low DOM concentration at S15, just upstream of the city of Caraz, followed by a peak just downstream of the city (S16). The increase in DOM downstream of Caraz could be related to the city's lack of sewage treatment.

The EEM-PARAFAC split between humic-like and protein-like components provides additional insights regarding DOM dynamics in the upper Santa watershed (Fig. 4). Except for S14 and S15, the results show a good agreement between FDOM and the humic-like substances, including for the two sampled tributaries. The non-detectable FDOM in proglacial lakes, where significant concentrations of DOC were measured, suggests that fluorescence is mainly of protein-like origin. The very low concentration in humic-like substances, even in Q3, which flows through large alpine meadows, can be explained by the low solubility of humic acids at pH lower than 5 (Wu et al., 2002). The significant amount of protein-like DOM in the pristine proglacial lakes of the Quilcay River can also be explained by the pH values. The waters of the upper Quilcay watershed have been described by Fortner et al. (2011) as very acidic and containing above-average metal concentrations arising from sulfide oxidation weathering, a process that is likely accelerated by bacterial mats. The high protein-like Fmax signal in the Quilcay River would therefore result from intense microbial activities.

In the Santa River, the differentiation between humic-like and protein-like substances shows that the very high DOC and FDOM values in Conococha lake are mainly of humic origin. In contrast, the EEM-PARAFAC method mainly associates variations in DOM concentration throughout the river's course with fluctuations in protein-like components, suggesting fluorescence of protein-like components as an indicator of anthropogenic influences on water quality.

3.2.4. Correlation study

As for Shullcas, a correlation study is performed to further explore the relation between the three different methods. Fig. 6b) and c) and d) shows regression study results in the same format as for Shullcas. With a Cook's distance of 100.5, S1 is the only sampling point overinfluencing regression outcomes. Fig. 6 therefore presents results from calculations made excluding that point and those including the point are given as a reference. The regression performed including S1 presents all R^2 values as systematically higher than those obtained excluding it. However, even when S1 is included, the correlation between DOC and the protein-like substances ($R^2 = 0.14$; p-value = 0.2), as well as the one between FDOM and the same substances ($R^2 = 0.12$; p-value = 0.23), is nonsignificant.

As observed on the scatter plots of Fig. 6, when S1 is excluded, correlations between DOC and Fmax values as well as between FDOM and Fmax values are all weak, regardless of the considered substances. The only correlation that is significant in that configuration is the one between DOC and FDOM ($R^2 = 0.64$; p-value = 0.89). As with Shullcas, regression line parameters differ greatly between when calculated including S1 and when not.

Both methods results show a good correlation with C1 and a poor one with those of the three other components. As seen earlier, C1 is identified as a humic-like component, while the three others are considered of protein-like origin.

4. Discussion

Studying DOM dynamics in two different glacierized watersheds of the tropical Andes provides an opportunity to compare the strengths and limitations of available measurement methods. DOC measurements carried out using the catalytic oxidation method have proven to be reliable in different environments. However, measuring organic carbon instead of organic matter can create discrepancies in results from other DOM estimation methods that

Table 2
Components identified in this study for the upper Santa basin with the corresponding wavelength position of its fluorescence maximum. Possible description is based on components identified in previous studies.

Component	λ (nm) (Ex/Em)	λ (nm) of possible analogue (Ex/Em)	Possible Source	Reference
C1	<255/440−490	260/380−460	Humic-like	Coble (1996)
		237−260/400−500	Humic-like	Bridgeman et al. (2011)
		255(350)/460	Terrestrial humic-like	Zhao et al. (2015)
		<255/448	Terrestrial humic-like	Stedmon and Markager (2005)
		250(340)/440	Terrestrial humic-like	Baghoth et al. (2011)
		<260/458	Terrestrial humic-like	Yamashita and Jaffé, (2008)
C2	295/335−360	225(290)/360	Autochthonous Tryptophan-like	Zhao et al. (2015)
		<250(290)/360	Amino acids or protein bounds	Baghoth et al. (2011)
		285/362	Non-humic-like	Yamashita and Jaffé, (2008)
C3	265(280)/320−350	275/340	Tryptophan-like, protein-like	Coble (1996)
		275/340	Tryptophan	Bridgeman et al. (2011)
		280/344	Tryptophan-like, autochthonous	Stedmon and Markager (2005)
C4	<250)/350	275/340	Protein-like, Tryptophan, Tyrosine	Bridgeman et al. (2011)
		275/340	Autochthonous Tryptophan-like	Zhao et al. (2015)
		280/344	Amino acids free or protein bounds	Baghoth et al. (2011)

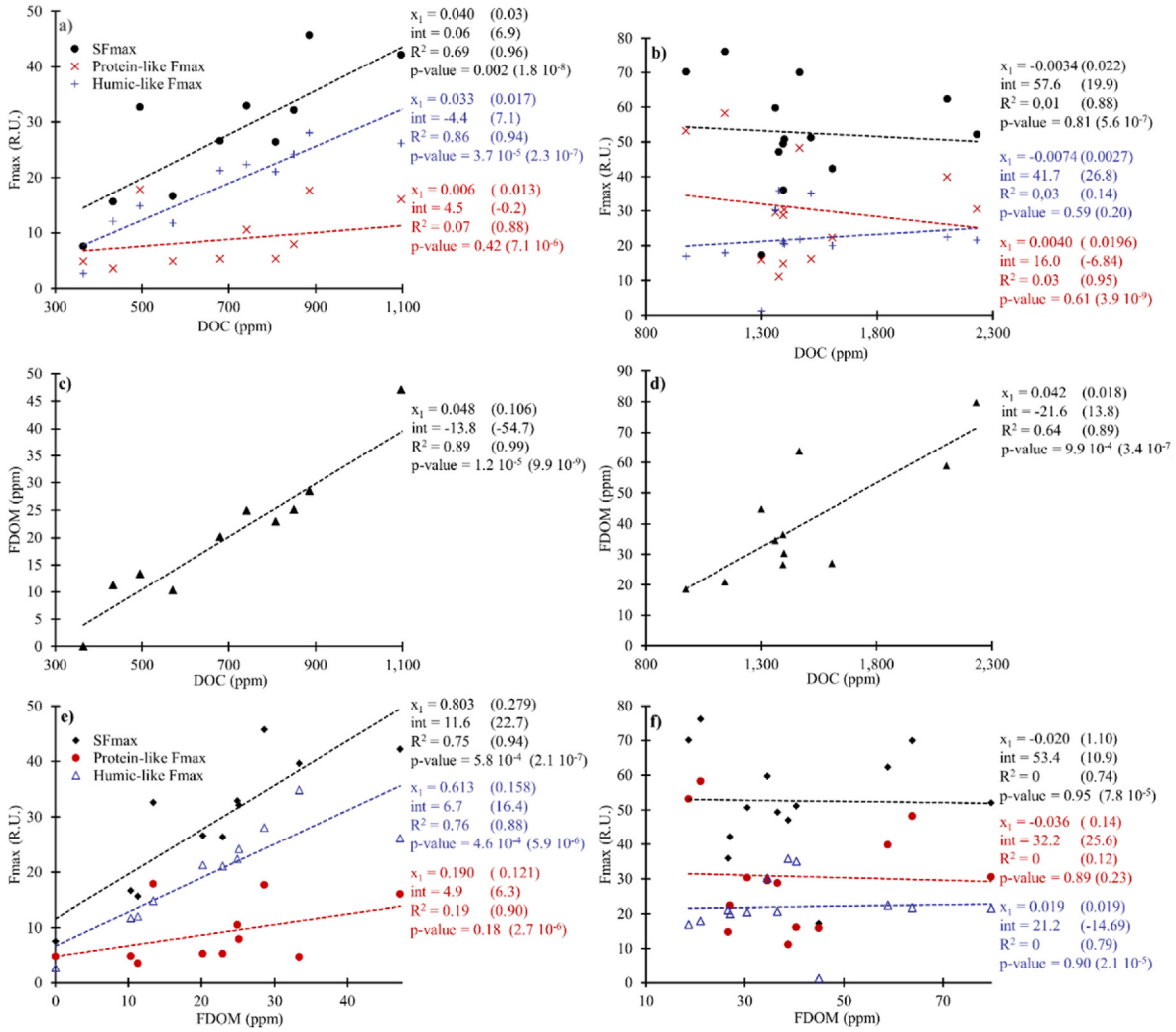

Fig. 6. Linear regression of methods results for the two main rivers; a), c) and e) apply to Shullcas while b), d) and f) apply to Santa. Figure a) and b) compare DOC results to EEN-PARAFAC; c) and d) compare DOC with FDOM; and e) and f) compare FDOM to EEM-PARAFAC. Plots and associated metrics correspond to dataset excluding overinfluencing points (Cook's distance over 1). Metrics calculated including those points are given in brackets.

might be difficult to quantify. As a benchtop laboratory method, it is not a direct *in-situ* measurement, and it requires sample pre-treatment due to the effects of air and light, among other factors. In addition, proteins are known to be difficult to oxidize (Rogowska-Wrzesinska et al., 2014), thus creating possible biases in the assessment of DOM dynamics when using DOC as a proxy for DOM. In our study, the lack of correlation observed between DOC concentrations and the protein-like substances' Fmax values at both sites could result from these oxidation difficulties.

The fluorometer equipped with a FDOM/CDOM sensor is a fast and efficient way to assess the DOM state at the watershed scale. FDOM profiles agree with DOC in the Shullcas watershed and in the first section of the upper Santa watershed, suggesting that this method could be used alone for characterization of DOM dynamics. However, the other studied areas show some limits to its use. The sensor wavelength only covers a fraction of the FDOM spectra and characterizes mainly humic-like substances. The limitations associated with the use of such narrow-spectrum FDOM sensors at our study sites were observed in spots with relatively low DOC concentrations and high proportions of protein-like substances. The systematic absence of a significant correlation between FDOM and the protein-like substances when outliers are excluded illustrates this limitation well. Disagreement between FDOM and EEM-PARAFAC methods was especially marked for samples S1 and L1 in the Shullcas watershed and P1, Q1, Q2, Q3 and Q4 in the Santa watershed. The missing spectra may be compensated by using a tryptophan sensor in addition to the one we used, but this option was not available in the present case. Other limitations arise from the sensitivity of FDOM to stream temperature, pH and turbidity, which requires monitoring of these characteristics in parallel to FDOM and eventually applying some corrections to the measurements.

The EEM-PARAFAC method allows for differentiation between humic-like and protein-like fluorescent substances and provides an estimate of DOM concentration through Fmax values. In the present study, EEM-PARAFAC provides key information for interpreting DOC and FDOM results. This was the case for understanding the difference in DOC and FDOM concentrations in proglacial lakes. In the Shullcas River, the fluctuation of the total fluorescence correlates well with the DOC concentration. In fact, the use of this method alone may have been enough to conduct the DOM dynamics assessment for that watershed. This is not the case in the upper Santa River, where differences in DOM variations among the three tested methods were observed on several occasions.

The combination of DOC, FDOM and fluorescence spectroscopy measurements allowed us to capture and understand DOM variations in both watersheds. The lack of sewage treatment systems in urban areas was clearly traced by the combined methods. Based on the study, the Shullcas watershed has a clear tendency for DOM concentration to increase as the water flows from the proglacial lakes to the urbanized area of Huancayo. The upper Santa DOM has a different behaviour, as the natural and anthropogenic loads of DOM become diluted by the river's confluence with numerous tributaries flowing from the Cordillera Blanca highlands. The study's results do not allow for the identification of a unique method that would provide as much information as the three combined. However, in this study, EEM-PARAFAC can be seen as the most valuable method for understanding DOM dynamics at the watershed scale. Discrepancies with other methods for the upper Santa River indicate that further studies are required before it can be recommended as a standalone solution. In addition, building the PARAFAC model has required a higher number of samples than what was required for the other methods, making that method more constraining to use.

The correlation study is characterized by important differences between the two studied watersheds. The agreement between DOC and FDOM is observed at each site but this is not the case when those methods are compared to the EEM-PARAFAC outputs. The Shullcas results exhibit a much stronger level of agreement between those methods and the EEM-PARAFAC than what is observed in the Santa watershed. Even where a significant coefficient of distribution is measured in both watersheds, the marked difference in regression line slopes indicates the relation between methods is probably site dependent.

To our knowledge, the present study represents a first attempt to compare FDOM, DOC and the EEM-PARAFAC methods for studying DOM dynamics targeting a use in the context of watershed water resources management. In that sense, findings will need to be confirmed through further studies. Different options for the FDOM measurements should be explored. For instance, the influence of turbidity on FDOM measurements, considered as negligible in the present study, should be investigated. The use of a sensor with wider spectral coverage or of a combination of different sensors can potentially improve the ability of this method to assess DOM dynamics at the watershed scale and therefore should also be explored. Finally, the site dependence of correlations between methods observed in the present study requires further study to be explained.

5. Conclusions

Comparing the performance of DOC, fluorescence spectroscopy and *in-situ* fluorometry to assess DOM dynamics in two glacierized watersheds of the tropical Andes allows us to identify the origins and magnitude of DOM loads. The results show that, in general, the Santa River presents higher DOM concentrations than the Shullcas River, with the exception of the measurements in the city of Huancayo, which present particularly high concentrations. The three methods were complementary to each other for assessing DOM dynamics at the scale of both watersheds, enabling their combination to meet the requirements of modern water resources management practices.

None of the methods taken individually achieved the same level of detail and accuracy as when the three methods were combined:

- The performance of the instruments used in this research suggests that, even if FDOM represents only a fraction of DOM, it captures dynamics that are to a certain extent comparable to those of the bulk DOM signal. However, at some points where a protein-like substance dominates the DOM composition, the method did not detect substantial DOM concentration.
- The FDOM/CDOM *in-situ* sensor used in the study has a bandwidth that is mainly situated in the humic part of the fluorescent fraction. Therefore, care must be taken when using such a sensor for the study of DOM dynamics because the measurement might miss protein-like FDOM that is found in wastewater. Other FDOM sensors on the market may present a different spectral coverage that includes the missing wavelengths. Further comparison of FDOM sensors at a watershed scale is still required.
- DOC measurements are a good reference for DOM dynamics. However, DOC is a carbon-specific fraction of DOM, and concentrations might differ. In addition, the correlation study suggested a limit exists in representing the protein-like fraction of the DOM, confirming difficulties already reported in the literature.
- 2 The EEM-PARAFAC method isolated three components in the Shullcas basin and four in the upper Santa basin. Identifying the components using previous literature studies allowed us to characterize the various fractions of DOM that fluoresce. Further research is needed to link total fluorescence to DOM concentration before making this method robust enough to study DOM dynamics throughout a watershed. An ANCOVA-type analysis could be considered to make progress in that direction.

CRediT authorship contribution statement

K.A. Rodriguez-Avella: Conceptualization, Methodology, Writing - original draft. **M. Baraer:** Supervision, Writing - review & editing. **B. Mark:** Writing - review & editing, Funding acquisition. **J. McKenzie:** Writing - review & editing. **L. Somers:** Investigation.

Declaration of competing interest

The authors declare that they have no known competing financial interests or personal relationships that could have appeared to influence the work reported in this paper.

Acknowledgements

This research is supported by the Geochemistry and Geodynamics Research Centre (GEOTOP) of Quebec, the Natural Science and Engineering Research Council (NSERC) of Canada and the National Science Foundation (NSF). The authors wish to thank Jesus Gomez, Eng., former Director of the Huascaran National Park, and Alejo C. Rapre, Director of the Autoridad Nacional del Agua office of Huaraz, for their active support in this research.

References

Anesio, A.M., Graneli, W., Aiken, G.R., Kieber, D.J., Mopper, K., 2005. Effect of humic substance photodegradation on bacterial growth and respiration in lake water. Appl. Environ. Microbiol. 71, 6267–6275.

Baghoth, S.A., Sharma, S.K., Amy, G.L., 2011. Tracking natural organic matter (NOM) in a drinking water treatment plant using fluorescence excitation–emission matrices and PARAFAC. Water Res. 45, 797–809.

Baker, A., Ward, D., Lieten, S.H., Pereira, R., Simpson, E.C., Slater, M., 2004. Measurement of protein-like fluorescence in river and waste water using a hand-held spectrophotometer. Water Res. 38, 2934–2938.

Baraer, M., Mark, B.G., McKenzie, J.M., Condom, T., Bury, J., Huh, K.-I., Portocarrero, C., Gómez, J., Rathay, S., 2012. Glacier recession and water resources in Peru's Cordillera Blanca. J. Glaciol. 58, 134–150.

Baraer, M., McKenzie, J., Mark, B.G., Gordon, R., Bury, J., Condom, T., Gomez, J., Knox, S., Fortner, S.K., 2015. Contribution of groundwater to the outflow from

ungauged glacierized catchments: a multi-site study in the tropical Cordillera Blanca, Peru. Hydrol. Process. 29, 2561–2581.
Bisutti, I., Hilke, I., Raessler, M., 2004. Determination of total organic carbon – an overview of current methods. TrAC Trends Anal. Chem. 23, 716–726.
Blaen, P.J., Khamis, K., Lloyd, C.E.M., Bradley, C., Hannah, D., Krause, S., 2016. Real-time monitoring of nutrients and dissolved organic matter in rivers: capturing event dynamics, technological opportunities and future directions. Sci. Total Environ. 569–570, 647–660.
Bolan, N.S., Adriano, D.C., Kunhikrishnan, A., James, T., McDowell, R., Senesi, N., 2011. Dissolved organic matter. In: Advances in Agronomy. Elsevier, pp. 1–75.
Booksh, K.S., Kowalski, B.R., 1994. Theory of analytical chemistry. Anal. Chem. 66, 782A–791A.
Bridgeman, J., Bieroza, M., Baker, A., 2011. The application of fluorescence spectroscopy to organic matter characterisation in drinking water treatment. Rev. Environ. Sci. Biotechnol. 10, 277.
Carstea, E.M., Bridgeman, J., Baker, A., Reynolds, D.M., 2016. Fluorescence spectroscopy for wastewater monitoring: a review. Water Res. 95, 205–219.
Chatterjee, A., Lal, R., Wielopolski, L., Martin, M.Z., Ebinger, M.H., 2009. Evaluation of different soil carbon determination methods. Crit. Rev. Plant Sci. 28, 164–178.
Chen, M., Li, C., Zeng, C., Zhang, F., Raymond, P.A., Hur, J., 2019. Immobilization of relic anthropogenic dissolved organic matter from alpine rivers in the Himalayan-Tibetan Plateau in winter. Water Res. 160, 97–106.
Coble, P.G., 1996. Characterization of marine and terrestrial DOM in seawater using excitation-emission matrix spectroscopy. Mar. Chem. 51, 325–346.
Coble, P.G., Spencer, R.G.M., Baker, A., Reynolds, D.M., 2014. Aquatic Organic Matter Fluorescence [WWW Document]. Aquat. Org. Matter Fluoresc. URL/core/books/aquatic-organic-matter-fluorescence/aquatic-organic-matter-fluorescence/0F72C6DF1C5D9231CE32F32B96714985. (Accessed 29 June 2019).
Conte, P., Kucerik, J., 2016. Water dynamics and its role in structural hysteresis of dissolved organic matter. Environ. Sci. Technol. 50, 2210–2216.
Cook, R.D., 1977. Detection of influential observation in linear regression. Technometrics 19 (1), 15–18.
Cory, R.M., Boyer, E.W., McKnight, D.M., 2011. Spectral methods to advance understanding of dissolved organic carbon dynamics in forested catchments. In: Levia, D.F., Carlyle-Moses, D., Tanaka, T. (Eds.), Forest Hydrology and Biogeochemistry. Springer Netherlands, Dordrecht, pp. 117–135.
Cross, P.C., Burnham, J., Leighton, P.A., 1937. The Raman spectrum and the structure of water. J. Am. Chem. Soc. 59, 1134–1147.
Derrien, M., Brogi, S.R., Gonçalves-Araujo, R., 2019. Characterization of aquatic organic matter: assessment, perspectives and research priorities. Water Res. 163, 114908.
DeVilbiss, S.E., Zhou, Z., Klump, J.V., Guo, L., 2016. Spatiotemporal variations in the abundance and composition of bulk and chromophoric dissolved organic matter in seasonally hypoxia-influenced Green Bay, Lake Michigan, USA. Sci. Total Environ. 565, 742–757.
Downing, B.D., Pellerin, B.A., Bergamaschi, B.A., Saraceno, J.F., Kraus, T.E.C., 2012. Seeing the light: the effects of particles, dissolved materials, and temperature on in situ measurements of DOM fluorescence in rivers and streams: effects and compensation for in situ DOM fluorescence. Limnol. Oceanogr. Methods 10, 767–775.
Fellman, J.B., Hood, E., Spencer, R.G.M., 2010. Fluorescence spectroscopy opens new windows into dissolved organic matter dynamics in freshwater ecosystems: a review. Limnol. Oceanogr. 55, 2452–2462.
Fortner, S., Mark, B., Mckenzie, J., Bury, J., Trierweiler, A., Baraer, M., Burns, P., Munk, L., 2011. Elevated stream trace and minor element concentrations in the foreland of receding tropical glaciers. Appl. Geochem. 26, 1792–1801.
Garreaud, R.D., 2009. The Andes climate and weather. Adv. Geosci. 22, 3–11.
Guittard, A., Baraer, M., McKenzie, J.M., Mark, B.G., Wigmore, O., Fernandez, A., Rapre, A.C., Walsh, E., Bury, J., Carey, M., French, A., Young, K.R., 2017. Trace-metal contamination in the glacierized Rio Santa watershed, Peru. Environ. Monit. Assess. 189.
Gurgiser, W., Juen, I., Singer, K., Neuburger, M., Schauwecker, S., Hofer, M., Kaser, G., 2016. Comparing peasants' perceptions of precipitation change with precipitation records in the tropical Callejón de Huaylas, Peru. Earth Syst. Dyn. 7, 499–515.
Hansen, A.M., Kraus, T.E.C., Pellerin, B.A., Fleck, J.A., Downing, B.D., Bergamaschi, B.A., 2016. Optical properties of dissolved organic matter (DOM): effects of biological and photolytic degradation: DOM optical properties following degradation. Limnol. Oceanogr. 61, 1015–1032.
Heiberger, R.M., Holland, B., 2004. Statistical analysis and data display: An intermediate course with examples in S-plus. Springer Texts in Statistic, NY.
Henderson, R.K., Baker, A., Murphy, K.R., Hambly, A., Stuetz, R.M., Khan, S.J., 2009. Fluorescence as a potential monitoring tool for recycled water systems: a review. Water Res. 43, 863–881.
Khamis, K., Sorensen, J.P.R., Bradley, C., Hannah, D.M., Lapworth, D.J., Stevens, R., 2015. In situ tryptophan-like fluorometers: assessing turbidity and temperature effects for freshwater applications. Environ. Sci. Process. Impacts 17, 740–752.
Introduction to fluorescence. In: Lakowicz, J.R. (Ed.), 2006. Principles of Fluorescence Spectroscopy. Springer US, Boston, MA, pp. 1–26.
Lawaetz, A.J., Stedmon, C.A., 2009. Fluorescence intensity calibration using the Raman scatter peak of water. Appl. Spectrosc. 63, 936–940.
Lee, E.-J., Yoo, G.-Y., Jeong, Y., Kim, K.-U., Park, J.-H., Oh, N.-H., 2015. Comparison of UV–VIS and FDOM sensors for in situ monitoring of stream DOC concentrations. Biogeosciences 12, 3109–3118.
Lee, M.-H., Osburn, C.L., Shin, K.-H., Hur, J., 2018. New insight into the applicability of spectroscopic indices for dissolved organic matter (DOM) source discrimination in aquatic systems affected by biogeochemical processes. Water Res. 147, 164–176.
Leenheer, J.A., Croué, J.-P., 2003. Peer reviewed: characterizing aquatic dissolved organic matter. Environ. Sci. Technol. 37, 18A–26A.
López-Moreno, J.I., Fontaneda, S., Bazo, J., Revuelto, J., Azorin-Molina, C., Valero-Garcés, B., Morán-Tejeda, E., Vicente-Serrano, S.M., Zubieta, R., Alejo-Cochachín, J., 2014. Recent glacier retreat and climate trends in Cordillera Huaytapallana, Peru. Global Planet. Change 112, 1–11.
Mark, B.G., McKenzie, J.M., Gómez, J., 2005. Hydrochemical evaluation of changing glacier meltwater contribution to stream discharge: Callejon de Huaylas, Peru/Evaluation hydrochimique de la contribution évolutive de la fonte glaciaire à l'écoulement fluvial: Callejon de Huaylas, Pérou. Hydrol. Sci. J. 50, 987.
Mark, B.G., Seltzer, G.O., 2003. Tropical glacier meltwater contribution to stream discharge: a case study in the Cordillera Blanca, Peru. J. Glaciol. 49, 271–281.
Massicotte, P., Asmala, E., Stedmon, C., Markager, S., 2017. Global distribution of dissolved organic matter along the aquatic continuum: across rivers, lakes and oceans. Sci. Total Environ. 609, 180–191.
Murphy, K.R., Hambly, A., Singh, S., Henderson, R.K., Baker, A., Stuetz, R., Khan, S.J., 2011. Organic matter fluorescence in municipal water recycling schemes: toward a unified PARAFAC model. Environ. Sci. Technol. 45, 2909–2916.
Murphy, K.R., Stedmon, C.A., Graeber, D., Bro, R., 2013. Fluorescence spectroscopy and multi-way techniques. PARAFAC. Anal. Methods 5, 6557.
Nikolaou, A.D., Meric, S., Lekkas, D.F., Naddeo, V., Belgiorno, V., Groudev, S., Tanik, A., 2008. Multi-parametric water quality monitoring approach according to the WFD application in Evros trans-boundary river basin: priority pollutants. Desalination 226, 306–320.
Old, G.H., Naden, P.S., Harman, M., Bowes, M.J., Roberts, C., Scarlett, P.M., Nicholls, D.J.E., Armstrong, L.K., Wickham, H.D., Read, D.S., 2019. Using dissolved organic matter fluorescence to identify the provenance of nutrients in a lowland catchment; the River Thames, England. Sci. Total Environ. 653, 1240–1252.
Peng, L., Yu, M., He, X.-S., Liu, S.-J., Zhang, P., 2018. Spectral characteristics of dissolved organic matter in landfill groundwater. Huan Jing Ke Xue Huanjing Kexue 39, 4556–4564.
Qualls, R.G., DeLaune, R.D., Reddy, K.R., Richardson, C.J., Megonigal, J.P., 2013. Dissolved organic matter. In: SSSA Book Series. Soil Science Society of America.
Rogowska-Wrzesinska, A., Wojdyla, K., Nedić, O., Baron, C.P., Griffiths, H.R., 2014. Analysis of protein carbonylation — pitfalls and promise in commonly used methods. Free Radic. Res. 48, 1145–1162.
Saraceno, J.F., Shanley, J.B., Downing, B.D., Pellerin, B.A., 2017. Clearing the waters: evaluating the need for site-specific field fluorescence corrections based on turbidity measurements. Limnol. Oceanogr. Methods 15, 408–416.
Stedmon, C.A., Bro, R., 2008. Characterizing dissolved organic matter fluorescence with parallel factor analysis: a tutorial: fluorescence-PARAFAC analysis of DOM. Limnol. Oceanogr. Methods 6, 572–579.
Stedmon, C.A., Markager, S., 2005. Resolving the variability in dissolved organic matter fluorescence in a temperate estuary and its catchment using PARAFAC analysis. Limnol. Oceanogr. 50, 686–697.
Stedmon, C.A., Markager, S., Bro, R., 2003. Tracing dissolved organic matter in aquatic environments using a new approach to fluorescence spectroscopy. Mar. Chem. 82, 239–254.
Sugimura, Y., Suzuki, Y., 1988. A high-temperature catalytic oxidation method for the determination of non-volatile dissolved organic carbon in seawater by direct injection of a liquid sample. Mar. Chem. 24, 105–131.
Sun, R., Wang, Z., Chen, L., Wang, W., 2013. Assessment of surface water quality at large watershed scale: land-use, anthropogenic, and administrative impacts. JAWRA J. Am. Water Resour. Assoc. 49, 741–752.
Suzuki, Y., Tanoue, E., Ito, H., 1992. A high-temperature catalytic oxidation method for the determination of dissolved organic carbon in seawater: analysis and improvement. Deep Sea Res. Part A. Oceanogr. Res. Pap. 39, 185–198.
Tang, J., Li, X., Cao, C., Lin, M., Qiu, Q., Xu, Y., Ren, Y., 2019. Compositional variety of dissolved organic matter and its correlation with water quality in peri-urban and urban river watersheds. Ecol. Indicat. 104, 459–469.
Thurman, E.M., 1985. Classification of dissolved organic carbon. In: Organic Geochemistry of Natural Waters. Springer Netherlands, Dordrecht, pp. 103–110.
UN-Water, 2008. Status Report on IWRM and Water Efficiency Plans for CSD16, p. 45. UN.
Wasswa, J., Mladenov, N., 2018. Improved temperature compensation for in situ humic-like and tryptophan-like fluorescence acquisition in diverse water types. Environ. Eng. Sci. 35, 971–977.
Wasswa, J., Mladenov, N., Pearce, W., 2019. Assessing the potential of fluorescence spectroscopy to monitor contaminants in source waters and water reuse systems. Environ. Sci. Water Res. Technol. 5, 370–382.
Watras, C.J., Hanson, P.C., Stacy, T.L., Morrison, K.M., Mather, J., Hu, Y.-H., Milewski, P., 2011. A temperature compensation method for CDOM fluorescence sensors in freshwater: CDOM temperature compensation. Limnol. Oceanogr. Methods 9, 296–301.
Weiwei, L., Xin, Y., Keqiang, S., Baohua, Z., Guang, G., 2019. Unraveling the sources and fluorescence compositions of dissolved and particulate organic matter (DOM and POM) in Lake Taihu, China. Environ. Sci. Pollut. Res. Int. 26, 4027–4040.
Wu, J., West, L., Stewart, D., 2002. Effect of humic substances on Cu(II) solubility in Kaolin-Sand soil. J. Hazard. Mater. 94, 223–238.
Yamashita, Y., Jaffé, R., 2008. Characterizing the interactions between trace metals and dissolved organic matter using excitation–emission matrix and parallel

factor analysis. Environ. Sci. Technol. 42, 7374–7379.
Yao, X., Wang, S., Ni, Z., Jiao, L., 2015. The response of water quality variation in Poyang Lake (Jiangxi, People's Republic of China) to hydrological changes using historical data and DOM fluorescence. Environ. Sci. Pollut. Res. 22, 3032–3042.
Yuan, K.-H., Zhong, X., 2008. Outliers, leverage observations, and influential cases in factor analysis: using robust procedures to minimize their effect. Socio. Methodol. 381, 329–368.
Zhang, Y., Liang, X., 2019. Understanding organic nonpoint-source pollution in watersheds via pollutant indicators, disinfection by-product precursor predictors, and composition of dissolved organic matter. J. Environ. Qual. 48, 102.
Zhao, Y., Song, K., Wen, Z., Li, L., Zang, S., Shao, T., Li, S., Du, J., 2015. Seasonal characterization of CDOM for lakes in semi-arid regions of Northeast China using excitation-emission matrices fluorescence and parallel factor analysis (EEM-PARAFAC). Biogeosci. Discuss. 12, 5725–5756.
Zhou, S., Chen, S., Yuan, Y., Lu, Q., 2015. Influence of humic acid complexation with metal ions on extracellular electron transfer activity. Sci. Rep. 5.
Zhou, Y., Wen, H., Liu, J., Pu, W., Chen, Q., Wang, X., 2019. The optical characteristics and sources of chromophoric dissolved organic matter (CDOM) in seasonal snow of northwestern China. Cryosphere 13, 157–175.